ISME

www.nature.com/ismej

ARTICLE

Desulfurivibrio spp. mediate sulfur-oxidation coupled to Sb(V) reduction, a novel biogeochemical process

Xiaoxu Sun[1,2], Tianle Kong[1,3], Fangbai Li[1,2], Max M. Häggblom[4], Max Kolton[1,2,5], Ling Lan[1,2], Maggie C. Y. Lau Vetter[6], Yiran Dong[7], Peng Gao[1,3], Joel E. Kostka[8,9], Baoqin Li[1,2] and Weimin Sun[1,2]✉

Antimony (Sb) contamination released from mine tailings represents a global threat to natural ecosystems and human health. The geochemical conditions of Sb tailings, which are oligotrophic and replete in sulfur (S) and Sb, may promote the coupled metabolism of Sb and S. In this study, multiple lines of evidence indicate that a novel biogeochemical process, S oxidation coupled to Sb(V) reduction, is enzymatically mediated by *Desulfurivibrio* spp. The distribution of *Desulfurivibrio* covaried with S and Sb concentrations, showing a high relative abundance in Sb mine tailings but not in samples from surrounding sites (i.e., soils, paddies, and river sediments). Further, the metabolic potential to couple S oxidation to Sb(V) reduction, encoded by a non-canonical, oxidative sulfite reductase (*dsr*) and arsenate reductase (*arrA*) or antimonate reductase (*anrA*), respectively, was found to be common in *Desulfurivibrio* genomes retrieved from metal-contaminated sites in southern China. Elucidation of enzymatically-catalyzed S oxidation coupled to Sb(V) reduction expands the fundamental understanding of Sb biogeochemical cycling, which may be harnessed to improve remediation strategies for Sb mine tailings.

The ISME Journal (2022) 16:1547–1556; https://doi.org/10.1038/s41396-022-01201-2

INTRODUCTION

Antimony (Sb) is a toxic metalloid widely distributed in the lithosphere and ranked as the ninth-most mined metal [1]. Sb is considered a priority pollutant by the United States Environmental Protection Agency [2], and the European Union [3]. The presence of Sb in the environment is mainly associated with sulfur (S) compounds, such as sulfide minerals (stibnite, Sb_2S_3), or oxides (valentinite, Sb_2O_3). Global production of Sb was approximately 160,000 metric tons in 2019, making Sb contamination a global concern across many major countries, such as Australia [4], Canada [5], and US [6]. China is the leading Sb mining country accounting for more than 80% of global production, which has caused severe Sb contamination in major mining areas across southern China [7]. Therefore, there is an urgent need to develop strategies for the remediation of sites contaminated with Sb mine tailings.

The biogeochemical transformation of Sb is primarily mediated by microbial oxidation and reduction processes [8, 9], which will in turn have a major impact on its fate and transport in the environment [10]. The mobility and toxicity of Sb strongly depend on its speciation [11], with Sb(III) being more toxic but less soluble compared to Sb(V) amongst the forms most commonly detected in situ [12]. Microbially mediated Sb(V) reduction has important environmental implications because its product, Sb(III), can be readily adsorbed to sulfide or Fe phases, which decreases its mobility. Understanding of biological Sb(V) reduction, however, remains in its infancy, with only a limited number of Sb(V)-reducing bacteria (SbRB) identified to date. Sb(V) reduction was first observed in anaerobic stibnite mine sediments from Idaho [13], and the process was further shown to be catalyzed by a pure culture of *Desulfuribacillus stibiiarsenatis* MLFW-2T, isolated from sediment of Mono Lake, California [14]. Recently, a respiratory antimonate reductase encoded by the *anrA* gene was suggested to catalyze Sb(V) reduction in *D. stibiiarsenatis* MLFW-2T [15]. Strain MLFW-2T is a heterotrophic bacterium that couples the oxidation of organic carbon substrates such as acetate with Sb(V) reduction. In contrast, it was reported that *Rhizobium* and *Methanosarcina* couple Sb(V) reduction to the oxidation of hydrogen or methane as electron donors, respectively, suggesting the potential for chemolithotrophic Sb(V) reduction [16, 17].

Chemolithoautotrophs are ubiquitously present in the environment and play essential roles in regulating the global biogeochemical cycles [18–21]. In particular, chemolithoautotrophic processes often predominate in oligotrophic environments, such as deep seafloor [22], subsurface [23], and groundwaters [24] ecosystems. Mine tailings, including Sb mine tailings, are typically oligotrophic metal-rich environments with elevated concentrations

[1]National-Regional Joint Engineering Research Center for Soil Pollution Control and Remediation in South China, Guangdong Key Laboratory of Integrated Agro-environmental Pollution Control and Management, Institute of Eco-environmental and Soil Sciences, Guangdong Academy of Sciences, Guangzhou 510650, China. [2]Guangdong-Hong Kong-Macao Joint Laboratory for Environmental Pollution and Control, Guangzhou Institute of Geochemistry, Chinese Academy of Sciences, Guangzhou 510640, China. [3]College of Environmental Science and Engineering, Donghua University, Shanghai 201620, China. [4]Department of Biochemistry and Microbiology, Rutgers University, New Brunswick, NJ 08901, USA. [5]French Associates Institute for Agriculture and Biotechnology of Drylands, Ben-Gurion University of the Negev, Beer Sheva, Israel. [6]Laboratory of Extraterrestrial Ocean Systems Institute of Deep-sea Science and Engineering, CAS, Sanya 572000, China. [7]School of Environmental Studies, China University of Geosciences (Wuhan), Wuhan 430074, China. [8]School of Biological Sciences, Georgia Institute of Technology, Atlanta, GA 30332, USA. [9]School of Earth and Atmospheric Sciences, Georgia Institute of Technology, Atlanta, GA 30332, USA. ✉email: wmsun@soil.gd.cn

Received: 12 September 2021 Revised: 3 January 2022 Accepted: 24 January 2022
Published online: 7 February 2022

of reduced S species introduced by sulfidic ores, such as stibnite [25]. The prevalence of S and limited organic carbon in tailings may hinder heterotrophic Sb(V) reduction while favoring chemolithotrophic metabolism. However, to our knowledge, this potentially important biogeochemical process was not previously demonstrated and past work has mainly focused on heterotrophic Sb(V)-reduction [13, 15, 26]. While evidence indicates that chemolithoautotrophic Sb(V) reduction is coupled to the oxidation of H_2 or CH_4 [16, 17], these electron donors are less relevant to severely contaminated tailing sites. Hence, we hypothesized that the autotrophic reduction of Sb(V) coupled to the oxidation of reduced S species as electron donor may represent a critical microbially mediated process in Sb mine tailings.

The objectives of this study were to combine biogeochemistry along with metagenomics to: (1) demonstrate the potential for Sb (V) reduction coupled to S oxidation, (2) elucidate the identity and metabolic potential of microorganisms mediating the process, and (3) investigate its significance in contaminated soils and sediments of southern China. Samples were collected from an Sb mine tailing site in Xikuangshan (XKS) in Southern China, where the world's largest Sb mine is located. Geochemical conditions in soils from the tailing sites were depleted in organic carbon but rich in S, thereby potentially favoring the growth of S-oxidizing SbRBs. Stable isotope probing (SIP), which has the potential to directly link microbial identity to function in complex environmental samples without isolation [27], was used to identify S-oxidizing SbRB. The metabolic potential was further explored through metagenomic-binning and microbial community analysis using 16 S rRNA gene amplicon sequencing. A flow chart summarizing the experimental approach is presented in Supplementary Fig. 1.

MATERIAL AND METHODS

Sample description

Samples were collected from the Sb-contaminated regions in Xikuangshan, Hunan, China (27°44′15″N, 111°27′46″). Four different sample types (15 replicates for each type) were collected, including Sb mine tailings (tailing), adjacent soil (soil), rice paddy (paddy), and river sediments (sediment) (Supplementary Fig. 2). These adjacent sites are located downstream of the Sb tailings site and have been affected by mining activities to varying extent. Surface soil was sampled with an ethanol-sterilized shovel, stored, and transported back to the laboratory on ice, where the samples were stored in a refrigerator at 4 °C for microbiological analysis within a month. The geochemical conditions of the samples are described in later sections.

Stable isotope probing (SIP) identification of S-oxidizing SbRB

Microcosms to promote the use of thiosulfate as the electron donor and antimonate (Sb(V)) as the electron acceptor were established with the XKS tailing samples. Either ^{13}C-labeled or ^{12}C-unlabeled bicarbonate were provided as the carbon source to identify the potential S-oxidizing SbRBs in the tailing samples. SIP incubations were prepared as follows: 1 gram of tailing samples was added as inoculum to 30 ml of mineral salts medium (MSM, pH = 7) (Supplementary Table 1). The enrichments were then purged with 99.9% N_2 gas to create an anoxic environment. The Sb+S treatment was supplied with 0.5 mM potassium pyroantimonate (99%, Macklin biochemical, Shanghai, China) and 0.5 mM sodium thiosulfate (99%, Macklin biochemical, Shanghai, China). Either 0.8 mM ^{13}C-labeled (99%, Cambridge Isotope Laboratories, MA, USA) or ^{12}C-unlabeled (99%, Macklin biochemical, Shanghai, China) sodium bicarbonate was added as a carbon source for ^{13}C-labeled treatment (^{13}C-Sb+S) and ^{12}C-unlabeled treatment (^{12}C-Sb+S), respectively. Additional controls without thiosulfate (No-S control) were prepared with 0.5 mM sodium antimonate and 0.8 mM ^{13}C-labeled (^{13}C-Sb) or ^{12}C-unlabeled (^{12}C-Sb) bicarbonate. The No-S controls were included to rule out the microbial populations using electron donors other than thiosulfate. A group of autoclaved controls were prepared to demonstrate that biological activities drove the process. All treatments and control cultures were prepared in triplicate for each sampling time point and incubated in the dark at 25 °C. The Sb(V) was re-spiked to all cultures after the complete removal of Sb(V) in Sb+S treatments on Day 27 of incubation. Changes to Sb speciation (i.e., Sb(III) and Sb(V)) in solution were monitored using liquid chromatography-atomic fluorescence spectrometry (LC-AFS) (AFS-9700, Haiguang, Beijing, China) following an established protocol [28]. The production of sulfate from thiosulfate oxidation was measured by ion chromatography (IC) (ICS-40, Dionex, CA, USA) following a published protocol [29].

At two time points (Day 27 and Day 45), the genomic DNA from both Sb +S treatments and both No-S controls (triplicate microcosms for each) were extracted using the DNeasy Powersoil Kit (Qiagen, Dresden, Germany) following the manufacturer's protocol. For each microcosm, the total volume was transferred to centrifuge tubes and the solids were pelleted by centrifugation at 924 g for 15 min at room temperature. The pellets were recovered after the supernatant was removed. For each microcosm, DNA from four parallel extractions (0.25 g wet weight of tailing sample for each extraction and 1 g total tailing sample per microcosm) was combined due to low DNA yields from tailing samples. Equal amounts of DNA (800 ng for each microcosm) were mixed with CsCl solution (1.714 g/mL) in a heat-sealable OpitSeal polypropylene tube (Beckman Coulter, Ca, USA) and centrifuged using an ultracentrifuge (Beckman Coulter, CA, USA) at 408,500 g for 40 h at 20 °C. The resulting stratified DNA-CsCl solution was fractionated into 18 aliquots (fractions) following the published protocol [30]. The buoyant density (BD) of each retrieved fraction was measured using a refractometer (Atago, Tokyo, Japan). The fractions were further purified, as previously described [31].

The DNA concentrations of the retrieved fractions were measured using Qubit (Invitrogen, CA, USA). The SSU rRNA (16 S rRNA), arsenate reductase (*arrA*), and antimonate reductase (*anrA*) genes were quantified for the selected fractions within the BD range 1.68–1.76 g/mL. Details of the qPCR primers and amplification procedures are available in Supplementary Table 2. The primer design procedures are available in the supplementary information.

The selected gradient fractions were further processed for SSU rRNA gene amplicon sequencing. For the ^{13}C- treatment, the fractions from the heavy (1.736–1.745 g/mL) and light (1.705–1.726 g/mL) layers were subjected to amplicon sequencing. For ^{12}C-Sb+S and No-S control, the light layers (1.705–1.726 g/mL) were sequenced. A total of 30 amplicon libraries were prepared.

Investigation of environmental samples

The tailing and other collected samples were analyzed to verify the environmental representativeness of the SIP identified S-oxidizing SbRB. A total of 60 environmental samples were analyzed (15 replicates for 4 different sample types, including tailings, soils, paddies, and sediments). DNA was extracted using a DNeasy Powersoil kit (Qiagen, Dresden, Germany) following the manufacturer's protocol. Geochemical parameters of these environmental samples were also characterized. For pH measurement, the 1 g freeze-dried soil samples were mixed with 10 ml distilled water and then measured by an HQ30d pH meter (Hach, CO, USA). The total organic carbon (TOC) was analyzed on a Vario MARCO cube elemental analyzer (Elementar, Hanau, Germany). The total Sb and As concentrations were analyzed on an LC-AFS (Haiguang, Beijing, China) after digestion with 5:1 (v/v) HNO_3 and HF. The water-soluble fractions of S (S), nitrogen (N) were extracted by mixing 2 g samples with 10 ml deionized water, and the supernatant was then analyzed on an Ion Chromatograph (ICS-40, Dionex, CA, USA).

Genomic DNA sequencing and analysis

For amplicon sequencing, the DNA was amplified with the primer set 515 F/806 R targeting the V4 hypervariable region of the 16 S rRNA gene [32, 33]. The details for the amplicon sequencing and sequence analysis are available in the supplementary information. The generated amplicon sequencing variants (ASVs) table were imported into the R package Phyloseq for downstream statistical analysis and visualization of the community compositions [34].

Shotgun metagenomic sequencing libraries were generated to reveal the metabolic potential of the putative S-oxidizing SbRBs identified by SIP. The attempt to directly sequence the heavy fractions of the ^{13}C-labeled treatments was unsuccessful due to the low amount of DNA available. Therefore, the overall genomic DNA from the ^{13}C-Sb+S treatment was sequenced on an Hiseq (Illumina, CA, USA) at Personal Biotechnology, Ltd. (Shanghai, China). One sequencing library from the SIP incubation was generated with 94,972,896 raw sequences (33 Gb). Details for the metagenome analysis are provided in the supplementary information.

The envMAGs (*Desulfurivibrio* MAGs retrieved from tailing environment metagenomes) of the SIP identified S-oxidizing SbRB were retrieved from the metagenomes of additional As/Sb contaminated environments,

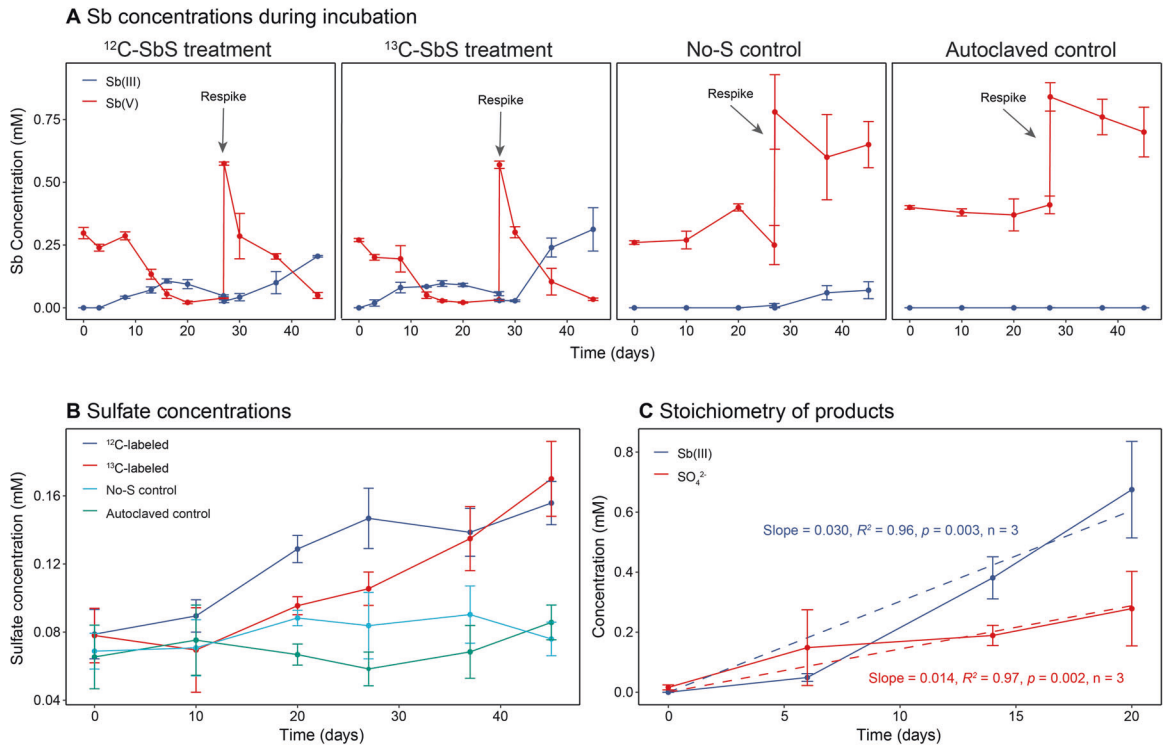

Fig. 1 Geochemical evidence of S-oxidizing Sb reduction. A The consumption of Sb(V) and the accumulation of Sb(III) during the SIP incubation in $^{12}C/^{13}C$-Sb+S treatments and No-S and autoclaved controls. **B** The accumulation of SO_4^{2-} during the SIP incubation. **C** The accumulation of products (Sb(III) and SO_4^{2-}) in transferred enrichment cultures for stoichiometry measurements.

including one metagenome from XKS tailings and metagenomes from three other metal-contaminated sites (Lanmuchang, LMC; Shimen, SM; and Qinglong, QL) (Supplementary Fig. 1). The retrieved sulfur-oxidizing SbRB MAG from enrichment cultures were used as a reference for mapping the metagenome reads and binning procedures. The retrieved environmental MAGs were imported into Anvi'o for panmetagenomic analysis [35]. Details regarding the assemble process of envMAGs is available in Supplementary Method 3.

Statistical analysis

The differences of microbial community structures among different sample types were estimated using PERMANOVA in R package Vegan [36]. The statistical differences of microbial populations and geochemical parameters among treatments and habitats were tested with a two-sided Welch's *T*-test of unequal variance in R. The contribution of geochemical parameters to the relative abundance of the *Desulfurvibrio* was predicted using a machine learning algorithm Random Forests (RF) prediction with the R package randomForest [37]. Briefly, the prediction was performed using the receiver operating characteristic approach [38] and visualized using partial dependence plots with MicrobiomeAnalyst [39].

RESULTS

Biogeochemical evidence for S-oxidation coupled to Sb(V) reduction

Stable isotope probing (SIP) was employed in enrichment cultures inoculated with Xikuangshan (XKS) tailings amended with reduced sulfur (thiosulfate) and Sb(V) ($KSb(OH)_6^-$) as well as either ^{12}C or ^{13}C bicarbonate as the sole carbon source. These chemicals have been previously used in S oxidation and Sb reduction studies, respectively [14, 40]. Control treatments without S (No-S control) or Sb (No-Sb control) addition, as well as autoclaved controls, were also prepared. During the incubation of the tailing microcosms, near complete removal of Sb(V) from the aqueous phase was only observed in the Sb+S treatments (Fig. 1A). Production of Sb(III) was observed in Sb+S treatments to a final concentration of 0.3 mM (s.d. = 0.1, $n = 6$). In contrast, Sb(V) reduction activity was not observed in either the No-S nor the autoclaved controls. Sulfate accumulated in the Sb+S treatments to a final concentration of 0.16 mM (s.d. = 0.003, $n = 6$) (Fig. 1B), which was significantly higher than that observed in the controls (0.08 mM, s.d. = 0.002, $p = 0.03$, df = 10). These observations indicate that microorganisms mediate the reduction of Sb(V) coupled to S oxidation in the Sb+S treatments. The overall stoichiometry of thiosulfate oxidation coupling to antimonate reduction can be described as follows:

$$4Sb(OH)_6^- + S_2O_3^{2-} + 2H^+ = 4Sb(OH)_3 + 2SO_4^{2-} + 7H_2O;\ \Delta G_0 = -390\,kJ/mol$$

where, ΔG_{f0} for $Sb(OH)_6^-$, $S_2O_3^{2-}$, $Sb(OH)_3$, SO_4^{2-}, and H_2O are −1208, −647, −513, −744, and −237 kJ/mol, respectively [41]. Reaction products accumulated in transferred enrichment cultures at the ratio of 2.1:1 (0.030 mM $Sb(OH)_3$/day and 0.014 mM SO_4^{2-}/day, Fig. 1C). Our experimentally-derived stoichiometry between the products (Sb(III) and SO_4^{2-}) was close to the theoretical ratio of 2:1.

Identification of S-oxidizing SbRB by DNA-SIP

Since microbial S-oxidation was implicated as the primary driver for Sb(V) reduction in this study, DNA-SIP was performed to identify putative S-oxidizing SbRB. Genomic DNA extracted from treatments ^{13}C-Sb+S, ^{12}C-Sb+S, ^{13}C-Sb, and ^{12}C-Sb at the two time points (day 27 and 45) were separated into "heavy" and "light" fractions according to their corresponding buoyant density (BD) by isopycnic gradient centrifugation. The abundance of SSU rRNA genes in the retrieved DNA fractions was quantified by qPCR. As shown in Fig. 2A, the highest abundance of SSU rRNA genes was observed in the light fractions (BD 1.705–1.726 mg/ml) at Day 27 in all samples. In the Day 45 samples, SSU rRNA genes were enriched in the heavy fractions (BD1.736–1.745 mg/ml; 273,000 ± 198,000 copies/g soil, $n = 9$, technical triplicates for each of the biological triplicates) in comparison to the light fractions (16,700 ± 8900 copies/g soil, $n = 9$, same as above) of the Sb+S treatments, thereby indicating the assimilation of labeled ^{13}C by putative

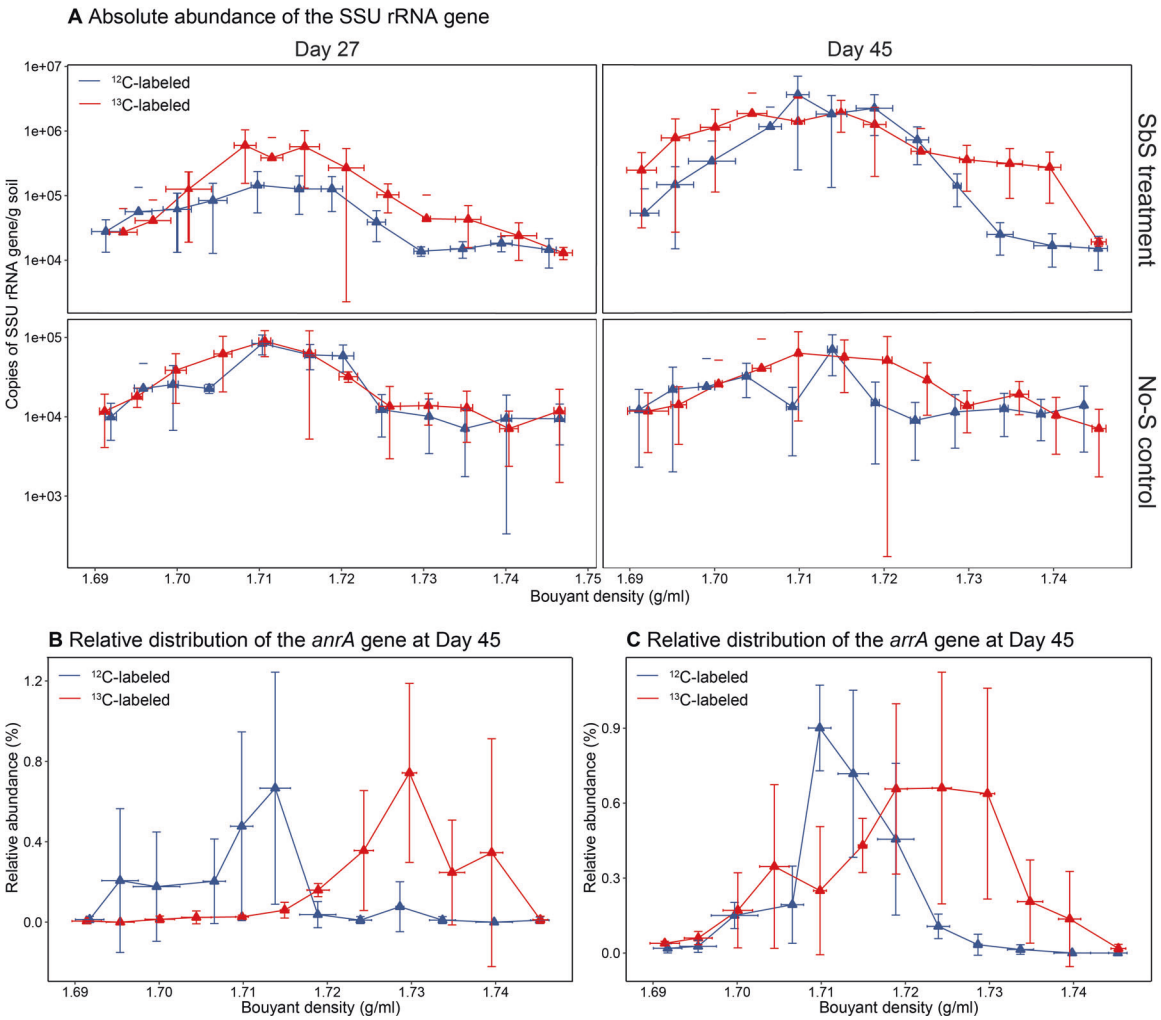

Fig. 2 Quantification of select genes in SIP incubation cultures. Abundance of the SSU rRNA (**A**), *anrA* (**B**), and *arrA* (**C**) gene copies in different SIP buoyant density fractions as determined by qPCR quantification.

S-oxidizing SbRB. In addition, putative genes encoding proteins in the Sb(V) reduction pathway, *arrA* and *anrA*, were also shown to be enriched in the heavy fractions compared to the light fractions of the Sb + S treatments on Day 45 (Fig. 2B, C).

Fractionated DNA was subjected to 16 S rRNA gene amplicon sequencing (Fig. 3). Sequencing was performed for the light and the heavy fractions of the ^{13}C-Sb+S treatments, while only the light fractions were analyzed for the ^{12}C-Sb+S and ^{12}C-Sb treatments. Only the heavy fractions were characterized for the ^{13}C-Sb samples. Whereas amplicon sequencing variants (ASVs) of *Desulfurivibrio* were dominant amongst the retrieved sequences from the heavy fractions of the ^{13}C-Sb+S treatment on day 45 (45.2 ± 4.1%, $n = 3$), this group comprised a minor proportion in the light fractions of the ^{12}C-Sb+S treatment (4.6 ± 4.6%, $n = 3$). The lower relative abundance of *Desulfurivibrio* in light fractions of the ^{12}C-Sb+S treatment was likely due to the presence of background microbial populations in tailing soil samples. In addition, *Desulfurivibrio* ASVs were not observed in the corresponding heavy fractions of the ^{13}C-Sb. The enrichment of *Desulfurivibrio* in the heavy fractions of the ^{13}C-Sb+S treatment suggests that this group contains the metabolic potential to couple S oxidation and Sb reduction.

Other microbial groups, including *Burkholderia-Coballeronia-Paraburkholderia* (11%, s.d. = 10 %, $n = 30$), *Ochrobactrum* (3.7%, s.d. = 6.6%, $n = 30$), and *Acinetobacter* (1.8%, s.d. = 2.1%, $n = 30$) showed a high relative abundance in nearly all treatments, suggesting that these taxa are not mediating S-oxidizing Sb(V) reduction processes. These microbial groups represent common reagent and laboratory contaminants that are known to affect sequencing results when the true biological target DNA concentrations are low [42]. Nonetheless, the presence of these groups did not interfere with the annotation of the SIP results, as their relative abundances were constant across all SIP fractions and were not enriched in the heavy fractions of the ^{13}C-Sb+S treatment. Thus, these groups were not discussed further.

Metagenomic evidence for the coupling of S oxidation and Sb reduction in *Desulfurivibrio*

Binning of metagenome sequences derived from S-oxidizing Sb(V) reducing enrichments was performed to retrieve *Desulfurivibrio* genomes and further characterize their metabolic potential. A total of 18 metagenome-assembled genomes (MAGs) were retrieved with > 50% completeness and < 10% redundancy (Supplementary Table 3), including three taxonomically affiliated with the *Deltaproteobacteria*. Among the retrieved MAGs, the 16 S rRNA gene of MAG04 was 100% identical to the dominant *Desulfurivibrio* ASV in SIP enrichment cultures. In addition, single copy gene taxonomy and taxonomic assignment of encoded genes each suggested that MAG04 is associated with the genus *Desulfurivibrio* (Supplementary Fig. 3). MAG04 showed high sequence identity to both *Desulfurivibrio alkaliphilus* AHT2, the representative strain of the genus, as well as to *Deltaproteobacteria* MLMS-1, a known S-oxidizing As(V) reducing bacteriaium (Supplementary Fig. 4). Further genome analysis of the

Fig. 3 Relative abundances of the dominant bacterial genera in different SIP fractions. Each dot represents the average abundance of the genus calculated from triplicate incubations.

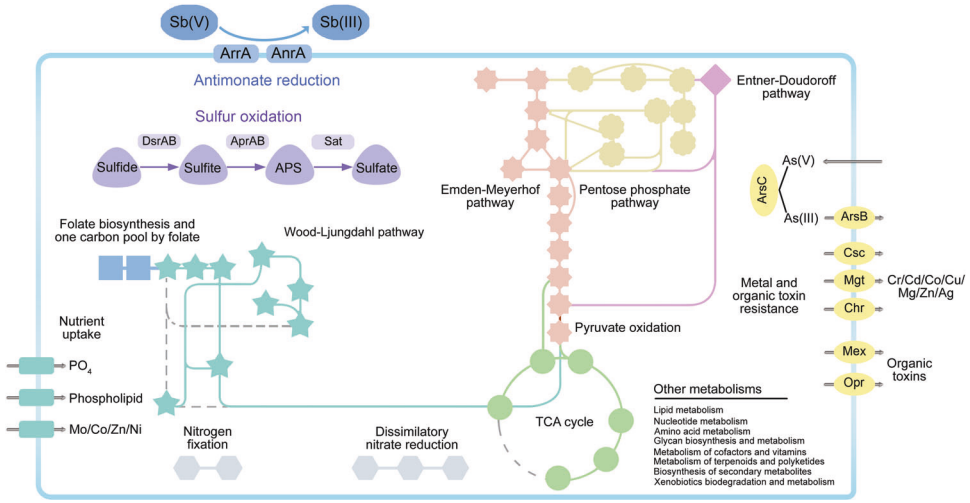

Fig. 4 Selected metabolisms encoded by the *Desulfurivibrio*-associated MAG-04. The genes were annotated using KEGG database. The dashed lines indicate missing genes.

metabolic potential of the *Desulfurivibrio* represented by MAG04 focused on S-oxidizing Sb(V) reduction, i.e., capacity for Sb(V) reduction, S oxidation, and C fixation.

Sb(V) reduction. Comparative genomics of MAG04 corroborated biogeochemical evidence to indicate the potential for Sb(V) and As(V) reduction (Supplementary Fig. 4). Specifically, MAG04-ORF-1029 was annotated as a member of the dimethyl sulfoxide reductase (DMSOR) family, showing a high amino acid sequence similarity (60%) and HMM bit score (1309.9) with the only known antimonate reductase (*anrA*) gene identified in the SbRB *Desulfuribacillus stibiiarsenatis* MLFW-2 [15]. In addition, an *anrA* gene was also detected in MAG09, which was associated with the family of *Bryobacteraceae* of the phylum *Acidobacterium*. MAG04-ORF-167 was identified as another member of the DMSOR family and a homolog to the arsenate reductase gene (*arrA*). The *blastp* results suggested MAG04-ORF-167 shares a high sequence identity (both at 80%) with the *arrA* sequence of known arsenate reducers *Geobacter* sp. OR-1 [43] and *Geobacter lovelyi*. Notably, the *arrA* gene was not detected in other retrieved MAGs.

S oxidation. *Desulfurivibrio*-associated MAG04 lacked genes encoding a canonical S oxidation (*sox)* pathway. Nevertheless, the MAG04 genome contained a complete gene set for sulfate reduction, including *sat*, *aprAB*, and *dsrAB* genes (Fig. 4). We propose that MAG04 contains non-canonical *dsr* that do not cluster with traditional reverse *dsr* genes. Rather, the *dsr* encoded by members of *Desulfobulbaceae* cluster within a branch of reductive *dsr* genes (Supplementary Fig. 5). Nonetheless, Dsr in members of the *Desulfobulbaceae* was reported to oxidize S for energy production and thereby referred to as non-canonical or oxidative-type *dsr* [40, 44, 45]. Additionally, a thiosulfate reductase (*phsA/psrA*) gene responsible for transformation of thiosulfate to sulfide and sulfite was also present in MAG04. In contrast, neither *sox* nor *dsr* were identified in the *anrA*-containing MAG09 genome nor in the available reference genomes associated with the family

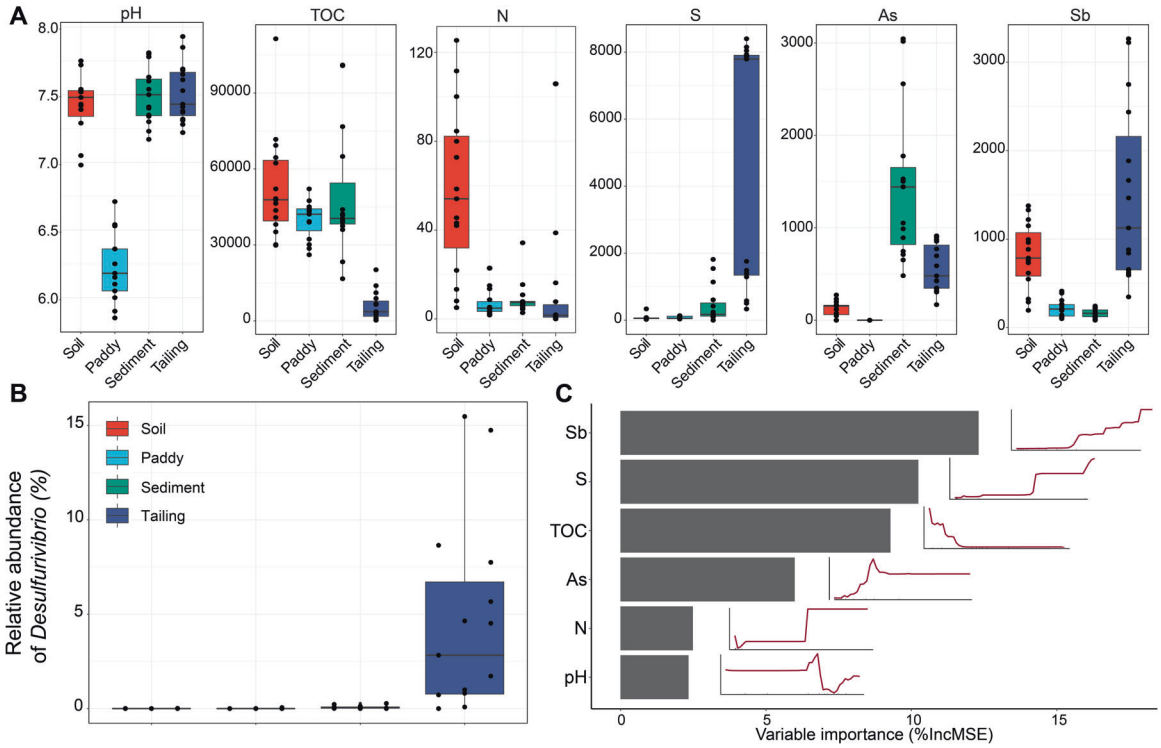

Fig. 5 The environmental distribution and geochemical controls of *Desulfurivibrio* spp. in the Sb contaminated Xikuangshan sites. A the geochemical properties of the XKS Sb mine tailing and adjacent sites (soil, paddy, and river sediments); **B** relative abundances of *Desulfurivibrio*; **C** the relative contribution of the geochemical variables on the distribution of the genus *Desulfurivibrio*. The units for panel are mg/kg soil, except for pH. The geochemical properties and *Desulfurivibrio* abundances were estimated based on 15 replicate samples of each type (tailing, soil, paddy, sediment).

Bryobacteraceae in the NCBI database (GCF_000702445.1 and GCF_015277775.1). Therefore, at this time, there is insufficient evidence to determine whether the *Bryobacteraceae*, which was represented by MAG09, is capable of S-oxidizing Sb reduction.

C fixation and other metabolisms. Multiple essential genes associated with C fixation pathways were present in *Desulfurivibrio*-associated MAG04 (Fig. 4). Although key genes for the reductive citrate cycle (rTCA cycle), including *korA*, which encodes the 2-oxoglutarate/2-oxoacid ferredoxin, and *porA*, which encodes a pyruvate ferredoxin oxidoreductase alpha subunit, were present in MAG04 [46], genes for the regeneration of the succinate and succinyl-CoA were absent. In contrast, a near complete gene set for the Wood-Ljungdahl pathway was identified in MAG04. Although genes encoding enzymes for the regeneration of formate (*fdhAB*) and subsequent 10-formyltetrahydrofolate (10-Formyl-THF; *fhs*) were absent, 10-Formyl-THF, however, might be replenished through the folate biosynthesis pathway and the subsequent one carbon pool by folate pathway.

In addition to the potential for autotrophic S metabolism, MAG04 also encoded complete gene sets for the Embden-Meyerhof pathway, pentose phosphate cycle, pyruvate oxidation, Entner-Doudoroff pathway, molybdate ABC transporter, nitrogen fixation pathway, and diverse metal and organic toxin resistance related genes (Fig. 4). Especially, the presence of complete dissimilatory nitrate reduction to ammonium (DNRA) genes indicates that the *Desulfurivibrio* populations represented by MAG04 could potentially use nitrate as an electron acceptor.

Environmental distribution of *Desulfurivibrio* spp. in Sb contaminated regions

Samples of Sb mine tailings (tailing), adjacent soil (soil), rice paddy (paddy), and river sediments (sediment) from nearby sites of the XKS region (15 replicates for sample type) were analyzed to assess the distribution of *Desulfurivibrio* spp. These sites were adjacent to the XKS tailing (within 1 km radius) and have been impacted by mining activities for centuries, making them suitable for investigating the geochemical controls of the *Desulfurivibrio* spp. Geochemical analysis revealed significantly elevated S and Sb concentrations in the tailings compared to the nearby impacted environments (soil, rice paddies, and riverine sediments) (Fig. 5A). Distinct microbial community composition was observed for each sample type (Fig. 5B and Supplementary Figs. 6–8). Putative S-oxidizing SbRB *Desulfurivibrio* showed a high relative abundance in mine tailings, while they were significantly less abundant in adjacent soils ($p = 0.004$, $df = 14$), paddies ($p = 0.004$, $df = 14$), and riverine sediments ($p = 0.004$, $df = 14$). Using the machine learning algorithm Random Forest (RF) prediction, measured geochemical parameters contributed 48% of the variation in the abundance of *Desulfurivibrio* ASVs. Specifically, soluble S concentration (12%) and total Sb concentration (11%) were revealed as major drivers of the ecological distribution of *Desulfurivibrio* (Fig. 5C).

Metabolic potential of soil-derived *Desulfurivibrio* MAGs

Four *Desulfurivibrio*-associated environmental MAGs (envMAGs, hereafter) were retrieved from soil metagenomes from four As- and Sb-contaminated sites (i.e., XKS, LMC, SM, and QL) located in the South China-circum-Pacific Sb ore belt. In addition, pangenomic analysis leveraged *Desulfurivibrio*-related genomes/MAGs from the NCBI database (Fig. 6 and Supplementary Table 4). The envMAGs were nearly identical to MAG04 (as indicated by ANI) with completeness varying between 70.4% to 88.7% and redundancy varying between 1.4–2.8%. In contrast, the envMAGs and MAG04 showed a lower sequence identity with other *Desulfurivibrio* genomes/MAGs retrieved from the NCBI database.

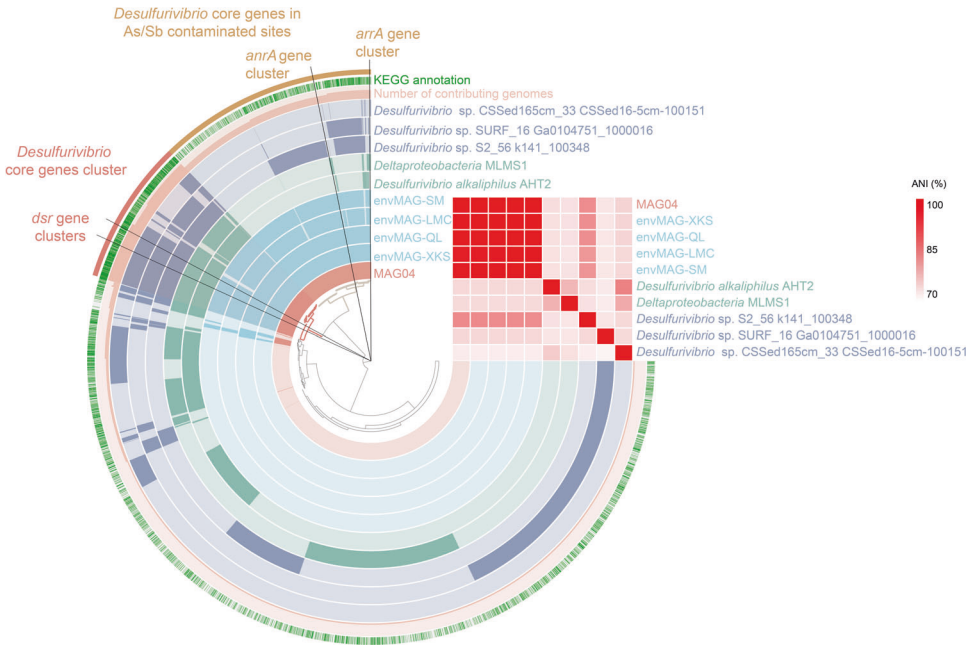

Fig. 6 The pangenomic analysis of *Desulfurivibrio* related genomes. The analyzed genomes include MAG-04, environmental *Desulfurivibrio* MAGs, and *Desulfurivibrio* genomes/MAGs retrieved from the NCBI database. The darker colors indicate the presence of gene clusters in each genome/MAG. The black lines connected to the center of the graph indicate the positions of the *dsrAB*, *anrA*, and *arrA* gene clusters. The number of contributing genomes indicates the number of genome/MAGs encoded the gene clusters. The *Desulfurivibrio* core genes cluster indicates the genes shared by all *Desulfurivibrio* genomes. The core genes in metal-contaminated sites indicate the genes encoded by the environmental MAGs retrieved from the four metal-contaminated sites (XKS, QL, LMC, SM). The KEGG annotation indicates whether the gene cluster can be annotated by KEGG database. The heat map represents the average nucleotide identity (ANI) between each pair of genomes (MAGs).

A group of shared genes, including those encoding oxidative-type *dsr*, pyruvate oxidation, phosphoribosyl diphosphate biosynthesis, and N-fixation, was identified across all *Desulfurivibrio* genomes/MAGs and is therefore proposed as a core gene cluster (Fig. 6). Moreover, a subset of genes was shared among the envMAGs and MAG04 retrieved from both As and Sb contaminated sites and regarded as *Desulfurivibrio* core gene cluster in As/Sb contaminated sites (Fig. 6). Genes (*anrA* and *arrA*) encoding for the Sb(V) reduction pathway were detected in all envMAGs and MAG04. Among *Desulfurivibrio*-related reference genomes/MAGS retrieved from NCBI, *Deltaproteobacteria* MLMS-1 encoded both the *anrA* and *arrA* genes, while *Desulfurivibrio* sp. S2_56 k141_100348 contained only the *arrA* gene.

DISCUSSION

Mine tailings are important sources of Sb contamination [47], and the dominance of the more mobile Sb(V) in tailings enhances its discharge, thereby increasing the potential to contaminate surrounding areas [48]. While Sb(III) is considered more toxic than Sb(V) [49], its lower solubility could constrain the contamination from impacting extended regions [11]. In addition to abiotic reactions [50], microbially mediated processes are considered as important factors for regulating the fate and transport of Sb in the environment [14]. Given the relatively low amounts of organic carbon available along with a high abundance of Sb(V) and reduced S, chemolithoautotrophic bacteria may play an important role in the fate and transport of Sb in tailings.

Microorganisms mediate the S-oxidizing Sb(V) reduction process

Multiple lines of evidence indicate that S-oxidizing Sb(V) reduction, a novel biogeochemical process, is mediated by indigenous microorganisms in tailing sites. Although to our knowledge S-oxidizing Sb(V) reduction was not previously reported, dissimilatory reduction of As, a metalloid with similar chemical properties, was shown to be coupled to S oxidation [45].

Desulfurivibrio spp. were identified as putative S-oxidizing SbRB by DNA-SIP. Members of *Desulfurivibrio* were first isolated from soda lakes [51] and have been later identified in other alkaline environments [52, 53]. Despite being reported in Sb contaminated soils [54, 55], *Desulfurivibrio* spp. were not previously implicated in Sb biogeochemical cycling.

A metagenomic approach was applied to S-oxidizing Sb(V)-reducing enrichment cultures to elucidate the metabolic potential of putative S-oxidizing SbRB. The recently proposed antimonate reductase gene, *anrA*, was found to be common to the genomes of diverse members of the *Deltaproteobacteria* [56], including *Desulfurivibrio*-associated MAG04. Given the similar chemistries of metalloids As and Sb, the As(V) reductase (ArrA) might also catalyze the reduction of Sb(V) [13, 57]. Enzymes responsible for As metabolism have often been implicated in the transformation of Sb [8]. For instance, the As(III) oxidase, AioA, can also function as a Sb(III) oxidase [58]. Similarly, the As resistance gene, *arsC*, was shown to increase bacterial resistance to Sb [59]. It has been hypothesized that dissimilatory Sb(V) reduction could be carried out by ArrA [13], which was confirmed by demonstrating that the deletion of *arrAB* genes in *Shewanella* sp. strain ANA-3 impaired its ability to reduce Sb(V) [57].

The oxidation of reduced S compounds is a favorable microbial metabolism in mining contaminated environments [60, 61]. It is suggested that *Desulfurivibrio* spp., and other members of the family *Desulfobulbaceae*, use a non-canonical oxidative-type *dsr* pathway to oxidize S rather than the *sox* pathway as reported previously [40, 44, 45]. In corroboration, oxidative-type *dsr* genes were shown to be highly conserved and clustered together compared to typical traditional reverse *dsr* (*rdsr*) and reductive-type *dsr* genes (Fig. 6 and Supplementary Fig. 5).

Given that mine tailings are often enriched in minerals and low in organic carbon, chemolithoautotrophy is prevalent [25]. Although further research is warranted, we provide evidence for C fixation coupled to Sb reduction. While MAG04 encoded a nearly complete set of Wood-Ljungdahl pathway genes, the missing *fdhAB* and *fhs* genes of the methyl branch may be due to incomplete binning procedures, as the close relatives of MAG04, *Deltaproteobacteria* MLMS-1 and *D. alkaliphilus* AHT-2, both encoded these genes [52]. Alternatively, *Desulfurivibrio*-associated MAG04 may employ a modified Wood-Ljungdahl pathway. The presence of the key gene *acsB* (acetyl-coenzyme A synthetase), which synthesizes acetyl-CoA from CO_2, and the subsequent *acsM* (Acyl-coenzyme A synthetase), which converts acetyl-CoA to acetate, provides further evidence that MAG04 has the capability to fix inorganic carbon into biomass. While *fdhAB* and *fhs* genes were missing, the regeneration of 10-formyl-THF could be accomplished through folate biosynthesis as an alternative pathway. The ability to use modified Wood-Ljungdahl pathway for C fixation has been previously reported in other microorganisms related to *Deltaproteobacteria* and *Chloroflexi* [62, 63].

Desulfurivibrio couples the S and Sb cycles in contaminated regions

Further analyses were performed to characterize the distribution of *Desulfurivibrio* and investigate its metabolic potential in Xikuangshan Sb mining impacted areas as well as other As- and Sb-contaminated sites. The genus *Desulfurivibrio* was identified as a dominant microbial taxon in the Xikuangshan tailings, which served as the inoculum for our DNA-SIP experiments. In contrast, its abundance was significantly lower in adjacent contaminated soil and sedimentary environments compared to their tailing counterparts (Fig. 5B). These adjacent sites were located downstream of the Sb mine in Xikuangshan, and suffered from contamination by either air deposition and/or surface runoff. As revealed by Random Forest predictions, the unique geochemical conditions present in tailing environments, which are depleted in organic carbon but replete in Sb and S, facilitate the dominance of *Desulfurivibrio* spp. compared to surrounding environments. In corroboration of our results, members of *Desulfurivibrio* were dominant in other Sb mine tailings [53, 55]. Furthermore, *Desulfurivibrio* spp. frequently inhabit environments with an active S cycle, such as soda lakes [44], the terrestrial subsurface [64], and oil sands [65]. Together, these observations suggest that *Desulfurivibrio* spp. are widely distributed in soil and sedimentary ecosystems and mediate the coupling of S and Sb geochemical cycles.

Pangenomic analysis was conducted to investigate relevant metabolic potentials of the *Deltaproteobacteria*, including MAG04, four envMAGs retrieved from As- and Sb-contaminated sites (XKS, QL, LMC, and SM), and NCBI-retrieved *Desulfurivibrio* genomes/MAGs. Genes for dissimilatory Sb reduction (*anrA*) were observed in MAG04, four envMAGs, and *Deltaproteobacteria* strain MLMS-1. Strain MLMS-1 was originally isolated from Mono Lake, CA, which is the same site where the Sb(V)-reducing *D. stibiiarsenatis* MLFW-2T was obtained. The presence of the *anrA* gene in MAGs/genomes retrieved from As and Sb contaminated sites indicates the ability to reduce Sb(V) may be a critical survival strategy adopted by *Desulfurivibrio* spp. in these As- and Sb-rich environments. In contrast, *anrA* was not detected in MAGs/genomes obtained from sites not exposed to As- and Sb-contamination. Genes encoding As reductase (*arrA*) were identified as part of the *Desulfurivibrio* core gene cluster detected in MAGs/genomes retrieved from As/Sb contaminated sites. Similar to the other two *arrA*-containing strains, MLMS-1 is from Mono lake, which contains an active As cycle, and *D.* sp. S2_56 k141_100348 originated from the deep-subsurface in Finland [64], which may also contain high As concentrations [66].

Oxidative-type *dsr* genes for sulfur oxidation were highly conserved among all *Desulfurivibrio*-associated genomes/MAGs (Supplementary Fig. 5), suggesting the importance of S oxidation for *Desulfurivibrio* spp. in the environment. Moreover, MAG04 encoded other traits that could potentially facilitate the growth and metabolism of *Desulfurivibrio* in oligotrophic mine tailings. For example, evidence indicates that MAG04 is capable of C fixation (Fig. 4). In addition, the presence of a nitrogen fixation gene cluster, *nifHDK*, and the high-affinity phosphate transporter gene cluster, *pstSABC*, point to the capability to scavenge necessary nutrients for growth. Therefore, our results suggest that autotrophic S-oxidizing Sb-reducing *Desulfurivibrio* spp. are primary producers that generate organic carbon and bioavailable nitrogen in tailings ecosystems.

Further understanding of the biogeochemical Sb cycle is critical for the successful management of Sb contaminated sites. Elucidation of the microbially mediated coupling of Sb reduction with S oxidation has important implications for the development of remediation strategies to prevent the release of Sb contamination from mine tailings into surrounding environments. We have shown that the genomes of putative S-oxidizing SbRB, *Desulfurivibrio* spp. reveal adaptation to the geochemical conditions of Sb mine tailings. *Desulfurivibrio*-like organisms are distributed throughout As- and Sb- contaminated sites across the South China-circum-Pacific Sb ore belt, which contains major Sb reserves in China [7]. Thus, we suggest that *Desulfurivibrio* should be further investigated as model organisms for harnessing S-oxidizing SbRB to facilitate future remediation of Sb mine tailings.

DATA AVAILABILITY

All the amplicon and metagenomic sequences were uploaded to the NCBI database under the bioproject number PRJNA678566. The *Desulfurivibrio*-MAG04 and the environmental MAGs are available in the NCBI database as biosample SAMN16879573-SAMN16879577. The geochemical data associated with the incubations are available in figshare (https://doi.org/10.6084/m9.figshare.15132546.v1).

REFERENCES

1. Scheinost AC, Rossberg A, Vantelon D, Xifra I, Kretzschmar R, Leuz AK, et al. Quantitative antimony speciation in shooting-range soils by EXAFS spectroscopy. Geochim Cosmochim Acta. 2006;70:3299–312.
2. United State Environmental Protection Agency. Priority pollutant list. 2014.
3. Council of the European Union. Council Directive 98/83/EC of 3 November 1998 on the quality of water intended for human consumption. 1998.
4. Warnken J, Ohlsson R, Welsh DT, Teasdale PR, Chelsky A, Bennett WW. Antimony and arsenic exhibit contrasting spatial distributions in the sediment and vegetation of a contaminated wetland. Chemosphere. 2017;180:388–95.
5. Beauchemin S, Kwong YTJ, Desbarats AJ, MacKinnon T, Percival JB, Parsons MB, et al. Downstream changes in antimony and arsenic speciation in sediments at a mesothermal gold deposit in British Columbia, Canada. Appl Geochem. 2012;27:1953–65.
6. Dovick MA, Arkle RS, Kulp TR, Pilliod DS. Extreme arsenic and antimony uptake and tolerance in toad tadpoles during development in highly591contaminated wetlands. Environ Sci Technol. 2020;54:7983–91.
7. He M, Wang X, Wu F, Fu Z. Antimony pollution in China. Sci Total Environ. 2012;421–422:41–50.
8. Filella M, Belzile N, Lett MC. Antimony in the environment: a review focused on natural waters. III. Microbiota relevant interactions. Earth-Sci Rev. 2007;80:195–217.
9. Li J, Wang Q, Oremland RS, Kulp TR, Rensing C, Wang G. Microbial antimony biogeochemistry: Enzymes, regulation, and related metabolic pathways. Appl Environ Microbiol. 2016;82:5482–95.
10. He M, Wang N, Long X, Zhang C, Ma C, Zhong Q, et al. Antimony speciation in the environment: Recent advances in understanding the biogeochemical processes and ecological effects. J Environ Sci (China). 2018;75:14–39.
11. Kong L, Hu X, He M. Mechanisms of Sb(III) oxidation by pyrite-induced hydroxyl radicals and hydrogen peroxide. Environ Sci Technol. 2015;49:3499–505.
12. Filella M, Belzile N, Chen YW. Antimony in the environment: A review focused on natural waters I. Occurence. Earth-Sci Rev. 2002;57:125–76.

13. Kulp TR, Miller LG, Braiotta F, Webb SM, Kocar BD, Blum JS, et al. Microbiological reduction of Sb(V) in anoxic freshwater sediments. Environ Sci Technol. 2014;48:218–26.
14. Abin CA, Hollibaugh JT. Dissimilatory antimonate reduction and production of antimony trioxide microcrystals by a novel microorganism. Environ Sci Technol. 2014;48:681–8.
15. Abin CA, Hollibaugh JT. Transcriptional response of the obligate anaerobe Desulfuribacillus stibiiarsenatis MLFW-2 T to growth on antimonate and other terminal electron acceptors. Environ Microbiol. 2019;21:618–30.
16. Lai CY, Wen LL, Zhang Y, Luo SS, Wang QY, Luo YH, et al. Autotrophic antimonate bio-reduction using hydrogen as the electron donor. Water Res. 2016;88:467–74.
17. Lai CY, Dong QY, Rittmann BE, Zhao HP. Bioreduction of antimonate by anaerobic methane oxidation in a membrane biofilm batch reactor. Environ Sci Technol. 2018;52:8693–8700.
18. Shi Y, Jiang Y, Wang S, Wang X, Zhu G. Biogeographic distribution of comammox bacteria in diverse terrestrial habitats. Sci Total Environ. 2020;717:137257.
19. Prosser JI The Ecology of Nitrifying Bacteria. *Biology Nitrogen Cycle*. 2007. Elsevier B.V., pp 223-43.
20. Kelly DP, Wood AP. The chemolithotrophic Prokaryotes. The Prokaryotes:Prokaryotic Communities and Ecophysiology. 2013. pp 275-87.
21. Walsh DA, Zaikova E, Howes CG, Song YC, Wright JJ, Tringe SG, et al. Metagenome of a versatile chemolithoautotroph from expanding oceanic dead zones. Science (80-). 2009;326:578–82.
22. Anantharaman K, Breier JA, Dick GJ. Metagenomic resolution of microbial functions in deep-sea hydrothermal plumes across the Eastern Lau Spreading Center. ISME J. 2016;10:225–39.
23. Emerson JB, Thomas BC, Alvarez W, Banfield JF. Metagenomic analysis of a high carbon dioxide subsurface microbial community populated by chemolithoautotrophs and bacteria and archaea from candidate phyla. Environ Microbiol. 2016;18:1686–703.
24. Jewell TNM, Karaoz U, Brodie EL, Williams KH, Beller HR. Metatranscriptomic evidence of pervasive and diverse chemolithoautotrophy relevant to C, S, N and Fe cycling in a shallow alluvial aquifer. ISME J. 2016;10:2106–17.
25. Sun X, Kong T, Häggblom MM, Kolton M, Li F, Dong Y, et al. Chemolithoautotrophic diazotrophy dominates the nitrogen fixation process in mine tailings. Environ Sci Technol. 2020;54:6082–93.
26. Nguyen VK, Lee JU. Isolation and characterization of antimony-reducing bacteria from sediments collected in the vicinity of an antimony factory. Geomicrobiol J. 2014;31:855–61.
27. Radajewski S, Ineson P, Parekh NR, Murrell JC. Stable-isotope probing as a tool in microbial ecology. Nature. 2000;403:646–9.
28. Viñas P, López-García I, Merino-Meroño B, Hernández-Córdoba M. Liquid chromatography-hydride generation-atomic fluorescence spectrometry hybridation for antimony speciation in environmental samples. Talanta. 2006;68:1401–5.
29. Zhao P, Niu J, Huan L, Gu W, Wu M, Wang G. Agar extraction from Pyropia haitanensis residue after the removal and purification of phycobiliproteins. J Appl Phycol. 2019;31:2497–505.
30. Neufeld JD, Vohra J, Dumont MG, Lueders T, Manefield M, Friedrich MW, et al. DNA stable-isotope probing. Nat Protoc. 2007;2:860–6.
31. Zhang M, Li Z, Haggblom MM, Young L, He Z, Li F, et al. Characterization of nitrate-dependent As(III)-oxidizing communities in arsenic-contaminated soil and investigation of their metabolic potentials by the combination of DNA-stable isotope probing and metagenomics. Environ Sci Technol. 2020;54:7366–77.
32. Caporaso JG, Kuczynski J, Stombaugh J, Bittinger K, Bushman FD, Costello EK, et al. QIIME allows analysis of high-throughput community sequencing data. Nat Methods. 2010;7:335–6.
33. Moonsamy PV, Williams T, Bonella P, Holcomb CL, Höglund BN, Hillman G, et al. High throughput HLA genotyping using 454 sequencing and the Fluidigm Access Array™ system for simplified amplicon library preparation. Tissue Antigens. 2013;81:141–9.
34. McMurdie PJ, Holmes S. Phyloseq: an R package for reproducible interactive analysis and graphics of microbiome census data. PLoS One. 2013;8:e61217.
35. Delmont TO, Eren EM. Linking pangenomes and metagenomes: the Prochlorococcus metapangenome. PeerJ. 2018;2018:1–23.
36. Oksanen J, Blanchet FG, Friendly M, Kindt R, Legendre P, McGlinn D, et al. vegan: Community Ecology Package. R package version 2.4-6. https://CRAN.R-project.org/package=vegan. 2018.
37. Liaw A, Wiener M. randomForest: Breiman and Cutler's random forests for classification and regression. R Packag version. 2015;4:6–10.
38. Díaz-Uriarte R, Alvarez de Andrés S. Gene selection and classification of microarray data using random forest. BMC Bioinforma. 2006;7:1–13.
39. Dhariwal A, Chong J, Habib S, King IL, Agellon LB, Xia J. MicrobiomeAnalyst: A web-based tool for comprehensive statistical, visual and meta-analysis of microbiome data. Nucleic Acids Res. 2017;45:W180–W188.
40. Müller H, Marozava S, Probst AJ, Meckenstock RU. Groundwater cable bacteria conserve energy by sulfur disproportionation. ISME J. 2020;14:623–34.
41. Sehmel GA. Cyanide and antimony thermodynamic database for the aqueous species and solids for the EPA-MINTEQ geochemical code. PNNL-6835; Pacific Northwest National Laboratory: Richland, WA, USA, 1989; pp 1–224.
42. Salter SJ, Cox MJ, Turek EM, Calus ST, Cookson WO, Moffatt MF, et al. Reagent and laboratory contamination can critically impact sequence-based microbiome analyses. BMC Biol. 2014;12:1–12.
43. Ohtsuka T, Yamaguchi N, Makino T, Sakurai K, Kimura K, Kudo K, et al. Arsenic dissolution from Japanese paddy soil by a dissimilatory arsenate-reducing bacterium Geobacter sp . OR-1. Environ Sci Technol. 2013;47:6263–71.
44. Thorup C, Schramm A, Findlay AJ, Finster KW, Schreiber L. Disguised as a sulfate reducer: Growth of the Deltaproteobacterium *Desulfurivibrio alkaliphilus* by sulfide oxidation with nitrate. MBio. 2017;8:1–9.
45. Hoeft SE, Kulp TR, Stolz JF, Hollibaugh JT, Oremland RS. Dissimilatory arsenate reduction with sulfide as electron donor: Experiments with Mono Lake water and isolation of strain MLMS-1, a chemoautotrophic arsenate respirer. Appl Environ Microbiol. 2004;70:2741–7.
46. Tersteegen A, Linder D, Thauer RK, Hedderich R. Structures and functions of four anabolic 2-oxoacid oxidoreductases in Methanobacterium thermoautotrophicum. Eur J Biochem. 1997;244:862–8.
47. Hiller E, Lalinská B, Chovan M, Jurkovič Ľ, Klimko T, Jankulár M, et al. Arsenic and antimony contamination of waters, stream sediments and soils in the vicinity of abandoned antimony mines in the Western Carpathians, Slovakia. Appl Geochem. 2012;27:598–614.
48. Casiot C, Ujevic M, Munoz M, Seidel JL, Elbaz-Poulichet F. Antimony and arsenic mobility in a creek draining an antimony mine abandoned 85 years ago (upper Orb basin, France). Appl Geochem. 2007;22:788–98.
49. Gebel T. Aresnic and antimony: Comparative approach on mechanistic toxicology. Chem Biol Interact. 1997;107:131–44.
50. Belzile N, Chen YW, Wang Z. Oxidation of antimony (III) by amorphous iron and Manganese oxyhydroxides. Chem Geol. 2001;174:379–87.
51. Sorokin DY, Tourova TP, Mußmann M, Muyzer G. Dethiobacter alkaliphilus gen. nov. sp. nov., and Desulfurivibrio alkaliphilus gen. nov. sp. nov.: Two novel representatives of reductive sulfur cycle from soda lakes. Extremophiles. 2008;12:431–9.
52. Melton ED, Sorokin DY, Overmars L, Chertkov O, Clum A, Pillay M, et al. Complete genome sequence of Desulfurivibrio alkaliphilus strain AHT2T, a haloalkaliphilic sulfidogen from Egyptian hypersaline alkaline lakes. Stand Genom Sci. 2016;11:1–9.
53. Liu JL, Yao J, Wang F, Min N, Gu JH, Li ZF, et al. Bacterial diversity in typical abandoned multi-contaminated nonferrous metal(loid) tailings during natural attenuation. Environ Pollut. 2019;247:98–107.
54. Liu J, Yao J, Sunahara G, Wang F, Li Z, Duran R. Nonferrous metal (loid) s mediate bacterial diversity in an abandoned mine tailing impoundment. Environ Sci Pollut Res. 2019;26:24806–18.
55. Xiao E, Krumins V, Tang S, Xiao T, Ning Z, Lan X, et al. Correlating microbial community profiles with geochemical conditions in a watershed heavily contaminated by an antimony tailing pond. Environ Pollut. 2016;215:141–53.
56. Shi LD, Wang M, Han YL, Lai CY, Shapleigh JP, Zhao HP. Multi-omics reveal various potential antimonate reductases from phylogenetically diverse microorganisms. Appl Microbiol Biotechnol. 2019;103:9119–29.
57. Wang L, Ye L, Jing C. Genetic identification of antimonate respiratory reductase in *Shewanella sp. ANA*-3. *Environ Sci Technol*. 2020;54:14107–13.
58. Wang Q, Warelow TP, Kang YS, Romano C, Osborne TH, Lehr CR, et al. Arsenite oxidase also functions as an antimonite oxidase. Appl Environ Microbiol. 2015;81:1959–65.
59. Butcher BG, Deane SM, Rawlings DE. The chromosomal arsenic resistance genes of Thiobacillus ferrooxidans have an unusual arrangement and confer increased arsenic and antimony resistance to Escherichia coli. Appl Environ Microbiol. 2000;66:1826–33.
60. Baker BJ, Banfield JF. Microbial communities in acid mine drainage. FEMS Microbiol Ecol. 2003;44:139–52.
61. Chen LX, Hu M, Huang LN, Hua ZS, Kuang JL, Li SJ, et al. Comparative metagenomic and metatranscriptomic analyses of microbial communities in acid mine drainage. ISME J. 2015;9:1579–92.
62. Zhuang WQ, Yi S, Bill M, Brisson VL, Feng X, Men Y, et al. Incomplete Wood-Ljungdahl pathway facilitates one-carbon metabolism in organohalide-respiring Dehalococcoides mccartyi. Proc Natl Acad Sci USA. 2014;111:6419–24.
63. Figueroa IA, Barnum TP, Somasekhar PY, Carlström CI, Engelbrektson AL, Coates JD. Metagenomics-guided analysis of microbial chemolithoautotrophic phosphite oxidation yields evidence of a seventh natural CO2 fixation pathway. Proc Natl Acad Sci USA. 2018;115:E92–E101.
64. Bell E, Lamminmäki T, Alneberg J, Andersson AF, Qian C, Xiong W, et al. Active sulfur cycling in the terrestrial deep subsurface. ISME J. 2020;14:1260–72.
65. Ramos-Padrón E, Bordenave S, Lin S, Bhaskar IM, Dong X, Sensen CW, et al. Carbon and sulfur cycling by microbial communities in a gypsum-treated oil sands tailings pond. Environ Sci Technol. 2011;45:439–46.

66. Lahermo P, Alfthan GWD. Selenium and arsenic in the environment in Finland. J Env Pathol Toxicol Oncol. 1998;17:205–16.

ACKNOWLEDGEMENTS

This work was supported by the National Natural Science Foundation of China (Grant Nos. U21A2035, 32161143018, 41907212, U20A20109, and 42107285), the Science and Technology Planning Project of Guangzhou (Grant No. 202002020072), GDAS' Project of Science and Technology Development (Grant Nos. 2020GDASYL-20200102018 and 2019GDASYL-0301002), Guangdong Basic and Applied Basic Research Foundation (Grant Nos. 2021A1515011374 and 2021A1515011461), High-End Foreign Experts Project (Grant No. G20200130015), the Science and Technology Planning Project of Guangdong Province (Grant Nos. 2019B121205006 and 2020B1212060048), and Guangdong Introducing Innovative and Entrepreneurial Talents (Grant No. 2017GC010570).

AUTHOR CONTRIBUTIONS

XS conceived and designed the experiment with input from WS, JEK, MMH and MK; WS acquired the funding needed to conduct the project. LL, TK, BL, and PG performed the field sampling and laboratory analyses; XS, TK performed the data analysis; and XS led writing the manuscript with close consultation with JEK, FL, MMH, MK, MCYLV, YD, and WS.

COMPETING INTERESTS

The authors declare no competing interests.

ADDITIONAL INFORMATION

Supplementary information The online version contains supplementary material available at https://doi.org/10.1038/s41396-022-01201-2.

Correspondence and requests for materials should be addressed to Weimin Sun.

Reprints and permission information is available at http://www.nature.com/reprints

Publisher's note Springer Nature remains neutral with regard to jurisdictional claims in published maps and institutional affiliations.